Molecular Dynamics Simulations of a Hydrated Protein Vectorially Oriented on Polar and Nonpolar Soft Surfaces

C. E. Nordgren,* D. J. Tobias,† M. L. Klein,* and J. K. Blasie*
*Department of Chemistry, University of Pennsylvania, Philadelphia, Pennsylvania, 19104-6323 USA; and †Department of Chemistry, University of California at Irvine, Irvine, California, 92697-2025 USA

ABSTRACT We present a collection of molecular dynamics computer simulation studies on a model protein-membrane system, namely a cytochrome *c* monolayer attached to an organic self-assembled monolayer (SAM). Modifications of the system are explored, including the polarity of the SAM endgroups, the amount of water present for hydration, and the coordination number of the heme iron atom. Various structural parameters are measured, e.g., the protein radius of gyration and eccentricity, the deviation of the protein backbone from the x-ray crystal structure, the orientation of the protein relative to the SAM surface, and the profile structures of the SAM, protein, and water. The polar SAM appears to interact more strongly with the protein than does the nonpolar SAM. Increased hydration of the system tends to reduce the effects of other parameters. The choice of iron coordination model has a significant effect on the protein structure and the heme orientation. The overall protein structure is largely conserved, except at each end of the sequence and in one loop region. The SAM structure is only perturbed in the region of its direct contact with the protein. Our calculations are in reasonably good agreement with experimental measurements (polarized optical absorption/emission spectroscopy, x-ray interferometry, and neutron interferometry).

INTRODUCTION

There is ongoing interest in the structural study of membrane proteins, and protein-membrane systems, to gain biological insight into the structure-function relationship of such complex systems, and to pave the way for the investigation of possible biomimetic devices. The peripheral membrane electron transfer protein, cytochrome *c*, has been studied extensively as one model of such systems; indeed, a great deal of experimental work has been done to characterize the structure of cytochrome *c* monolayers on organic films (Pachence and Blasie, 1987, 1991; Pachence et al., 1989, 1990; Amador et al., 1993; Chupa et al., 1994; Wang et al., 1994; Delamarche et al., 1995; Edmiston et al., 1997; Wood et al., 1997; Edwards et al., 2000; Kneller et al., 2001).

When chemisorbed to self-assembled monolayers (SAMs) that include thiol endgroups, yeast cytochrome *c* can form vectorially oriented protein films, due to covalent disulfide bonding between a thiol endgroup and the unique surface cysteine residue of the cytochrome *c*. This property, coupled with the possibility of moving the unique cysteine residue to other locations on the protein surface via site-directed mutagenesis, makes this system very useful for the investigation of directional charge transport across a protein film.

However, due to the fact that protein-membrane systems are in general not crystalline, experimental structural determinations are unable to provide three-dimensional structural information at atomic resolution. We would like to answer such questions as: What is the true chemical character of the surface presented by the exposed endgroups of the SAM? How and where does the SAM affect the structure of the protein molecule? How and where does the protein affect the SAM structure? To address these questions, we shall investigate structural properties of this system (e.g., the orientation of the protein with respect to the normal to the SAM surface and the atomic resolution structure along the normal to the monolayer plane) via computer simulation, and compare these results with relevant experimental measures (e.g., polarized optical absorption/emission spectroscopy and x-ray and neutron interferometry). If the simulations are in agreement with the experimental information that is available (which is generally limited in both dimension and resolution), then we may have some confidence that these same simulations will provide accurate three-dimensional structural information at the atomic level.

This study is a substantial extension of previous work done by Tobias et al. (1996) to provide for a much better correlation with extant experimental information. The earlier work provided the first molecular dynamics simulations describing the effects of the interaction of cytochrome *c* with both polar and nonpolar SAM surfaces but in the absence of hydrating water. In that study, it was found that the interactions in the case of the polar SAM had substantially larger effects on the structure of the protein and the SAM than for the nonpolar case. In the current work, most importantly, we have added water to the system, to model varying degrees of hydration of the protein. We have used improved models for the coordination of the heme iron atom, namely both six-coordinate and five-coordinate (i.e., with and without, respectively, a covalent bond between the

Submitted September 29, 2001, and accepted for publication April 25, 2002.

Address reprint requests to J. Kent Blasie, 231 South 34th Street, Philadelphia, PA 19104-6323. Tel.: 215-898-6208; Fax: 215-573-2046; E-mail: jkblasie@sas.upenn.edu.

0006-3495/02/12/2906/12 $2.00

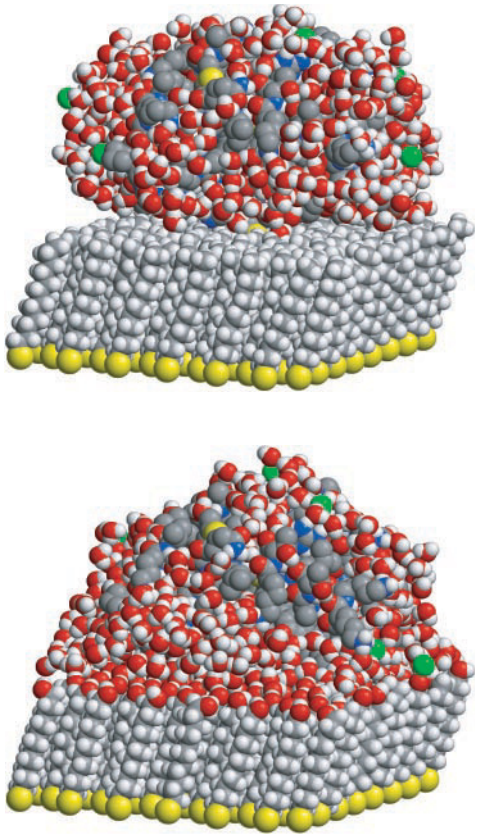

FIGURE 1 Representative instantaneous snapshots of the two canonical simulation systems: "nonpolar-wet" (*upper*) and "polar-wet" (*lower*). The color scheme is: carbon in gray, hydrogen in white, nitrogen in blue, oxygen in red, sulfur in yellow, chloride in green, and iron in magenta.

iron atom and its sulfur axial ligand). We have also used a different model for the polar SAM, with a mixture of thiol and hydroxyl endgroups, to provide for a soft polar surface without the long-range electrostatic interactions provided by charged endgroups. Finally, we have done some preliminary investigation of the effects of temperature on the structure and dynamics of this system. Overall, this study provides insight into the balance between protein-solvent and protein-surface interactions in determining the functionally important details of the structure and fluctuations of a peripheral membrane protein (e.g., see Edwards et al., 2000).

MATERIALS AND METHODS

Model systems

A variety of simulation systems were considered, but two systems, denoted "nonpolar-wet" and "polar-wet," were the canonical model systems to which all of the other variations will be compared (Fig. 1). In each of these two systems, a single molecule of yeast cytochrome *c* is present along with a set of 96 $S(CH_2)_{11}X$ alkanethiol chain molecules. The chains are close-packed in a 6 by 8 array with two chains per unit cell. In the "nonpolar-wet" system, we have 95 chains with the endgroup $X{=}{=}CH_3$, and these methyl endgroups cause the "upper" surface of the SAM to be nonpolar (hydrophobic). On the other hand, for the "polar-wet" system, we have 95 chains with X═OH, and these hydroxyl endgroups cause the "upper" surface of the SAM to be polar (hydrophilic) but uncharged. For both systems, the last remaining chain (located roughly in the center of the SAM) has the endgroup X═SH. This thiol endgroup was used for the attachment of the overlying protein molecule via a disulfide bond to the sulfur atom of its unique surface cytsteine residue. At the "lower" surface of the SAM (farthest from the protein), each chain has a sulfur headgroup added; these were constrained (by a strong radial harmonic potential) to remain essentially in a planar triangular lattice, to model the chemisorption of the SAM to a solid substrate. Additionally, to make the system electroneutral, six chloride ions were added to the system. As described so far, these two model systems are very similar to those reported in earlier work (Tobias et al., 1996). But in the present case, 500 water molecules were also added to each system, to hydrate the protein and the SAM; a six-coordinate iron model was also used.

TABLE 1

System name	SAM type	Temperature	Hydration	Heme model
Nonpolar-wet	Nonpolar	300 K	500 Waters	Standard
Polar-wet	Polar	300 K	500 Waters	Standard
Nonpolar-cold	Nonpolar	263 K	500 Waters	Standard
Polar-cold	Polar	263 K	500 Waters	Standard
Nonpolar-damp	Nonpolar	300 K	100 Waters	Standard
Polar-damp	Polar	300 K	100 Waters	Standard
Nonpolar-nosulfur	Nonpolar	300 K	500 Waters	5-Coordinate
Polar-nosulfur	Polar	300 K	500 Waters	5-Coordinate
Solution-dense	No SAM	300 K	500 Waters	Standard
Solution-sparse	No SAM	300 K	500 Waters	Standard
Polar-crystal	Polar	300 K	500 Waters	Standard

Beyond these two canonical systems, several additional systems were also simulated with permutations of various system parameters (Table 1). In one case, two simulations were performed (denoted "nonpolar-cold" and "polar-cold") that were identical to the canonical pair, except that instead of performing the simulation at room temperature (300 K), a lower temperature (263 K) was used. Another variation (called "nonpolar-damp" and "polar-damp") was to run each of the two systems with only 100 molecules of water present. In another case ("nonpolar-nosulfur" and "polar-nosulfur"), we used an altered model for the coordination of the iron atom in the heme group of the protein with the sulfur axial ligand unbonded. In yet another variation ("polar-static"), which was done for the case of the protein on the uncharged-polar SAM, the covalent disulfide bond between the SAM and the protein was not used; rather the system was allowed to evolve with only electrostatic and other nonbonded interactions between the protein and the SAM. Finally, we also ran a pair of simulations ("solution-dense" and "solution-sparse") that included one protein molecule and 500 water molecules, as in the canonical systems, but did not include a SAM.

For the SAMs, we used an all-atom potential model that reproduces very well the structure of liquid alkanes (Tobias et al., 1997). Thiol groups were modeled with the explicit hydrogen potential of Jorgensen (1986). The protein and the SAM hydroxyl groups were modeled with the "polar H" CHARMM PARAM19 potential (Reiher, 1985). For the waters, we used the TIP3P model (Jorgensen et al., 1983). For the chloride ions, the potential of Buckner and Jorgensen (1989) was used.

One important point to mention is that the CHARMM force field does not include parameters for the interaction of iron with sulfur; thus, although sufficient for modeling such heme proteins as myoglobin, we found it necessary to augment the CHARMM parameter set to model cytochrome *c*. As we were unable to locate any spectroscopic data relevant to the iron-sulfur bond (T. Spiro, personal communication, Princeton University, 1999), we simply used the same force constants as for the iron-nitrogen

TABLE 2

System name	Initial conditions	Trajectory length
Nonpolar-wet	Crystalline	1500 ps
Polar-wet	Nonpolar-wet @ $t = 600$ ps	900 ps
Nonpolar-cold	Crystalline	1500 ps
Polar-cold	Nonpolar-cold @ $t = 600$ ps	900 ps
Nonpolar-damp	Crystalline	1500 ps
Polar-damp	Nonpolar-damp @ $t = 600$ ps	900 ps
Nonpolar-nosulfur	Crystalline	1200 ps
Polar-nosulfur	Crystalline	1200 ps
Solution-dense	Crystalline	1500 ps
Solution-sparse	Crystalline	1500 ps
Polar-crystal	Crystalline	1500 ps

bond. The iron-sulfur equilibrium bond length, meanwhile, was specified to be 2.35 Å, in accord with the x-ray crystal structure (Louie and Brayer, 1990). Under physiological conditions, the iron atom in cytochrome *c* is six-coordinate, as in the x-ray crystal and NMR solution structures; however, it is known (Edwards et al., 2000) that the iron-sulfur bond is relatively weak and can be broken under certain experimental conditions. (In the earlier work of Tobias et al. (1996), a five-coordinate iron model was used.)

The systems were intended to model intrinsically two-dimensional monolayer systems; however, it was found that a two-dimensional Ewald summation method (Hautman and Klein, 1992) for the electrostatic forces was actually unstable, owing to the fact that the atoms present in the molecular dynamics (MD) box were distributed as widely in the *z* direction (normal to the monolayer) as in the monolayer plane. Thus, fully three-dimensional Ewald summation (for the electrostatic forces) and minimum-image periodic boundary conditions (for the van der Waals forces) were used. However, the height of the MD box was made large enough (90 Å, which was roughly twice the physical extent of the system along that direction) that no significant effects on the structure were caused by the *z* periodicity. The dimensions of the MD box in the *x* and *y* directions (i.e., in the plane of the SAM) were 43.98 by 44.88 Å. The van der Waals forces were spherically truncated at a 10-Å radius (Allen and Tildesly, 1989). For the special case of the two runs without a SAM ("solution-dense" and "solution-sparse"), three-dimensional periodic boundaries and Ewald summation were also used but with a 60-Å cubical MD box.

Initial conditions

The initial conditions used for the various simulation runs were of two types: most systems were started from crystalline coordinates; whereas, for computational expediency, a few systems were begun using the preequilibrated structure of another simulation as their starting point (Table 2). All of the systems with the nonpolar SAM, as well as the "polar-nosulfur" and "polar-crystal" systems, were begun from crystalline coordinates, as follows: The initial coordinates of the SAM were created based on the crystal structure of methyl stearate (Aleby and von Sydow, 1960), keeping 12 methyl units from the stearoyl chain. The initial coordinates of the protein were taken from the x-ray crystal structure (Protein Data Bank file 1YCC; Louie and Brayer, 1990); four internal water molecules from this structure were also retained. The six added chloride ions were initially placed near surface lysine groups of the protein. The waters were initially placed by superimposing a block of preequilibrated bulk water (2560 molecules) over the system, deleting those waters that overlapped other atoms and then deleting all the remaining waters except for the 500 (or 100), which were closest to the protein. After this setup, a brief energy minimization was applied to the entire system, and then dynamics were begun.

The two simulations done in the absence of a SAM were begun similarly. The initial protein configuration was again taken from the x-ray crystal structure. In one run ("solution-dense") the waters were initially placed in the immediate vicinity of the protein (in the same fashion as for the nonpolar SAM systems, as described above), whereas in the other run ("solution-sparse"), the waters were spread evenly throughout the otherwise-empty volume of the MD box with random orientations at the start of the simulation.

For the sake of efficiency, three simulations ("polar-wet," "polar-cold," and "polar-damp") were initiated from trajectories in progress ("nonpolar-wet," "nonpolar-cold," and "nonpolar-damp," respectively; see again Table 2). In each case, the polar-SAM system was started from the coordinates of the corresponding nonpolar-SAM trajectory at $t = 600$ ps; the SAM endgroups were simply changed from methyls to hydroxyls, and the dynamics were restarted. To assess the validity of this approach, one of these systems was later redone, starting from the crystalline initial conditions as described above; the only difference between the "polar-wet" and "polar-crystal" systems was the choice of initial conditions.

Equilibration and dynamics

For the dynamics calculations on these systems, the CHARMM program (version 23; Brooks et al., 1983) was used. We used a timestep of 1.0 fs, and SHAKE (Ryckaert et al., 1977) was used to constrain all covalent bonds to hydrogen atoms. The simulations were done in the NVT ensemble, using Nosé-Hoover chains (Martyna et al., 1992) to maintain the temperature. Separate thermostats were used for the protein, the SAM, and the waters. For each system component, the thermostat chain length was five; the fictitious masses of the thermostat variables were chosen by the method of Martyna et al. (1992) with time scales of 0.5 ps. As noted above, all of the simulations were performed at room temperature (300 K) except for two ("nonpolar-cold" and "polar-cold"), which were done at 263 K.

The various simulated systems were each allowed ample time for equilibration, after which dynamics were continued and statistics were collected. The temperature of each system required well under 100 ps to stabilize. The heme angle and radius of gyration of the protein (see below in the Results and Discussion) took between 100 and 600 ps to settle (Fig. 2). The redistribution of the water required the most time to equilibrate: typically, from 600 to 800 ps of time was needed (Fig. 3). It is also clear that the water structure had an important influence upon the structure of the rest of the system. For the systems with only 100 waters present, the protein structural parameters were equilibrated after only ~200 ps; this fact led us to our choice of starting several of the simulations from closely-related trajectories in which the water was already equilibrated.

In the end, each of the systems was run for well over a nanosecond (Table 2) of total simulation time. The computations were performed on SGI R10000 workstations and servers at the University of Pennsylvania; the simulations required as much as 4 CPU-months apiece to run a full 1500-ps trajectory.

RESULTS AND DISCUSSION

In Table 3, we present the results of some numerical analyses of the protein structure from various MD trajectories. In the first column, we report the radius of gyration of the protein. In the second column, we report the root-mean-square deviation of the protein backbone in the MD structure as compared with the x-ray crystal structure of cytochrome *c* (Louie and Brayer, 1990), which was, in each case, the initial protein structure used for the MD trajectory. In the third column, we report the "heme angle" of the protein, which we define to be the angle between the normal

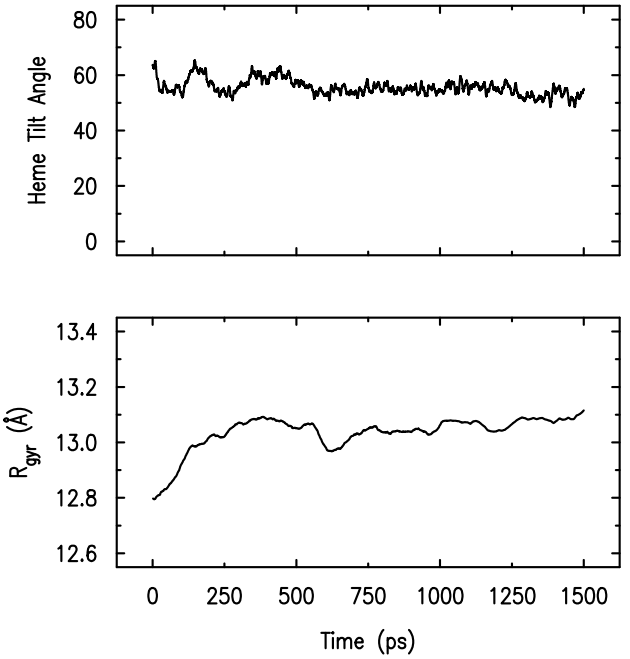

FIGURE 2 "Heme tilt-angle" and radius of gyration, as a function of MD trajectory time, for the "nonpolar-wet" system.

vector to the plane of the protein's heme group and the normal vector to the plane of the SAM. In the fourth column, we report the protein's eccentricity for selected cases. In each case, the reported numbers are averages over the final 400 to 500 ps of the corresponding MD trajectory with the standard deviation of the quantity reported as an uncertainty.

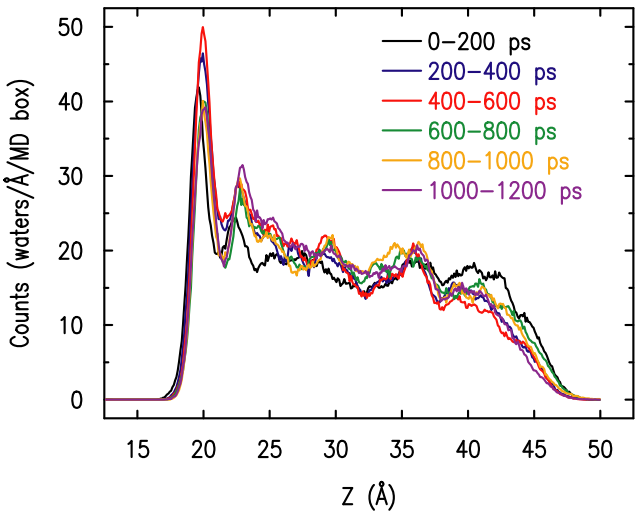

FIGURE 3 Sequence of water profiles for the "nonpolar-wet" system. Each curve is a histogram of the distribution of water molecule z-coordinates, averaged over a different 200-ps block of the MD trajectory.

Radius of gyration and eccentricity

The radius of gyration (R_{gyr}) for a system of particles is defined as the mass-weighted geometric mean of the distance of each particle from the system's center of mass. The eccentricity is defined as $(1 - I_{max}/I_{ave})$ in which I_{max} is the maximal principal moment and I_{ave} is the average of the three principal moments of inertia for a system of particles. We compute these two quantities for all the atoms (and psuedoatoms) of the protein, including the heme group, to characterize the overall "size" and "shape" of the protein, respectively. For reference, it should be pointed out that the values of the R_{gyr} and the eccentricity for the x-ray crystal structure of cytochrome *c* (i.e., the initial protein structure in each of these simulations) are 13.0 and 0.18 Å, respectively.

One can see that there is a small but consistent difference in the R_{gyr} value between pairs of systems that differ only in the polarity of the SAM surface. Comparing "nonpolar-wet" versus "polar-wet," "nonpolar-damp" versus "polar-damp," and "nonpolar-nosulfur" versus "polar-nosulfur," the proteins on polar SAMs had a R_{gyr} roughly 1% larger. At lower temperature (comparing "nonpolar-cold" versus "polar-cold"), we find the R_{gyr} to be ~2% larger on the polar SAM. Comparing "polar-crystal" versus "nonpolar-wet," which had fully equivalent initial conditions, we see a 3% larger R_{gyr} with the polar SAM. These results are consistent with the earlier findings by Tobias et al. (1996) of the R_{gyr} being 2% larger for the polar-SAM system.

Turning our attention now specifically to the effect of hydration, it appears that greater amounts of water produce larger values of the R_{gyr}. For the "wet" systems (with 500 water molecules per protein molecule) at room temperature, the protein's R_{gyr} is ~2% larger (on both types of SAM) than that for the "damp" systems (with 100 water molecules per protein molecule). In the case of our "nosulfur" systems (with a five-coordinate heme iron and 500 waters per protein), the R_{gyr} was ~3% larger (on both types of SAM) than that found by Tobias et al. (1996) with the same heme model but no hydration.

These observations may be explained by the following argument: in a near-vacuum environment (such as the low-hydration simulations) a protein experiences "electrostriction," that is, the polar sidechains on the surface tend to collapse inward and interact with other parts of the protein; on the other hand, in the presence of protein-protein contacts (such as in a protein crystal) or protein-solvent interactions (e.g., in a protein crystal, or in the fully hydrated simulations), or protein-surface interactions (such as a protein in contact with a polar-endgroup SAM), the polar sidechains of a given protein molecule may extend away from its surface and interact with external polar groups. As seen above, the protein is larger when attached to a surface than when floating free in solvent, the protein is larger on a polar surface than on a nonpolar surface, and the protein is larger when fully hydrated than when not hydrated. From

TABLE 3

System name	R_{gyr} (Å)	RMSDX (Å)	Heme angle (°)	Eccentricity
Nonpolar-wet	13.07 ± 0.03	2.07 ± 0.07	53.7 ± 3.0	0.21
Polar-wet	13.21 ± 0.05	2.06 ± 0.08	53.5 ± 3.0	0.23
Nonpolar-cold	13.21 ± 0.04	2.10 ± 0.07	56.1 ± 3.2	
Polar-cold	13.46 ± 0.09	2.63 ± 0.18	56.3 ± 2.4	
Nonpolar-damp	12.77 ± 0.04	1.82 ± 0.03	57.0 ± 2.6	
Polar-damp	12.92 ± 0.03	2.01 ± 0.04	61.4 ± 2.2	
Nonpolar-nosulfur	13.20 ± 0.05	2.63 ± 0.09	48.4 ± 2.8	
Polar-nosulfur	13.39 ± 0.10	2.45 ± 0.15	60.0 ± 3.1	
Solution-dense	12.88 ± 0.02	1.48 ± 0.07	N/A	
Solution-sparse	12.89 ± 0.01	1.99 ± 0.08	N/A	
Polar-crystal	13.41 ± 0.04	2.14 ± 0.08	61.9 ± 2.5	0.23
Nonpolar-dry*	12.8	3.2	36	0.20
Polar-dry*	13.0	2.9	66	0.24

*Taken from Tobias et al., 1996.

the numerical results obtained here, it appears that protein-SAM interactions have a larger effect than hydration, in terms of increasing the protein's radius of gyration.

Another interesting observation is the effect of temperature upon the R_{gyr}. It is apparent that one result of lowering the system temperature from 300 to 263 K is to make the protein larger (by ~1% on a nonpolar SAM and 2% on a polar SAM). This result is somewhat surprising, because proteins do not normally exhibit negative thermal expansion, at least in relatively isotropic environments (Frauenfelder et al., 1987). However, this effect could be the result of the anisotropic environment seen by our model protein upon a SAM surface, or might simply be an artifact of using the (radially symmetric) radius of gyration to characterize the structure of a protein in such an intrinsically two-dimensional environment.

Finally, we consider the effect of the coordination number of the heme iron atom. Comparing the "wet" systems with the "nosulfur" systems, one can see that the R_{gyr} is ~1% larger when the sulfur axial ligand is unbonded. Also, the R_{gyr} found for the two systems simulated in the absence of a SAM ("solution-dense" and "solution-sparse," with six-coordinate iron) is ~2% larger than the value (12.6 Å) found by Tobias et al. (1996) for a simulation of an unhydrated cytochrome *c* molecule alone in vacuum (with five-coordinate iron); this is consistent with a 3% increase in the R_{gyr} upon hydration (as seen above), mitigated by a 1% decrease in the R_{gyr} due to bonding the heme iron atom to its sulfur axial ligand. Similarly, our "wet" systems exhibited R_{gyr} values ~2% greater than those of the "dry" systems of Tobias et al. (1996).

The differences in overall size of the protein for these different systems described above, as measured by the radius of gyration, are also similarly manifest in the shape of the protein as measured by its eccentricity, as calculated for some selected cases. In particular, the eccentricity of the hydrated protein on the uncharged-polar SAM surface is 9% to 10% larger, irrespective of the differing initial conditions ("polar-wet" and "polar-crystal"), than for the protein on the nonpolar SAM surface ("nonpolar-wet"), whereas the eccentricities for the protein on either of the nonpolar or polar SAM surfaces is 17% to 28% larger, respectively, than for cytochrome *c* in single crystals. Similarly, these effects of the protein's environment on the overall shape of the protein are also dependent on the hydration of the protein, the eccentricity for the protein on the uncharged-polar SAM surface ("polar-dry") being ~20% larger than for the protein on the nonpolar SAM surface ("nonpolar-dry") in the absence of water, compared with the smaller 9% to 10% difference in the presence of water.

Deviations of protein backbone from crystal structure

In the second column of Table 3, we report the root mean square deviations (RMSD) of the simulated protein structures from the x-ray crystal structure (i.e., the initial coordinates used for the protein in each simulation), calculated using only the coordinates of the backbone α-carbons, and herein referred to as the "RMSDX." One can see that one-half of the simulated systems have an RMSDX value of 2.0 Å within uncertainties. However, there are notable exceptions to this common value: 1) the "polar-cold" system has an RMSDX ~30% larger; 2) the "nonpolar-damp" system has an RMSDX ~10% smaller; 3) the "solution-dense" system has an RMSDX ~25% smaller; and 4) the two "nosulfur" systems have an RMSDX ~30% larger.

First, we observe the effect of the heme iron coordination model on the RMSDX. Comparing the canonical "wet" systems with the "nosulfur" systems, we see that in the absence of the iron-sulfur covalent bond, the RMSDX increases markedly (19% on the polar SAM and 27% on the nonpolar SAM). This is certainly reasonable, because breaking the iron-sulfur bond allows a certain amount of relaxation in the spatial structure of the protein with the Met-85 residue no longer constrained to stay near the iron atom.

Next, let us consider the effect of the SAM surface polarity on the secondary structure of the protein. For the canonical pair of systems ("nonpolar-wet" and "polar-wet"), as well as the "polar-crystal" system, there is no significant difference in the RMSDX; however, at lower temperature or at lower hydration, the protein on the polar SAM shows a greater deviation from the crystal structure than does the protein on the nonpolar SAM. For the pair of systems at 263 K, the difference in RMSDX values is ~25%, whereas for the pair of systems with only 100 waters of hydration, there is a 10% difference. This would seem to indicate that the effects of SAM surface polarity upon the structure of the attached protein molecules can be reduced by either: 1) an increase of the mobility of the hydrating water at higher temperature; or 2) screening of the protein-SAM nonbonded interactions by the presence of a larger

amount of water. In contrast, for the systems with a five-coordinate iron model, the opposite trend was found. Comparing the two "nosulfur" systems, the RMSDX was ~7% larger in the nonpolar-SAM system; similarly, in the earlier work by Tobias et al. (1996), the RMSDX was ~10% higher in the "nonpolar-dry" system than in the "polar-dry" system.

Additionally, the deviations from the crystal structure found in the two "dry" systems were significantly larger than for any of the systems studied in the present work. Besides the obvious dependence on the iron coordination model, we attribute this to the influence of hydration on the system. That is, it would seem that the presence of water helps to maintain a simulated protein structure more akin to the crystal structure. Either or both of two factors may account for this: 1) with hydration, the protein experiences surface interactions more similar to those present in a crystal (i.e., protein-protein and protein-water contacts) than it does in vacuum; and 2) the water molecules serve to screen some of the influence of the SAM surface upon the protein structure. In fact, it should be noted that the "damp" systems actually exhibit an RMSDX slightly smaller than that found for the "wet" systems; this may indicate that the choice of 100 waters per protein is close to the "right" number to provide the protein with intermolecular interactions that mimic those within a protein crystal. The RMSDX values for our "nosulfur" systems (on each SAM type) lie midway between the corresponding values for our "wet" systems and for the "dry" systems of Tobias et al. (1996). This seems to indicate that hydrating the system and using a six-coordinate iron model are both equally important to the simulated secondary structure of the protein.

One additional curious result bears mentioning here. For the two systems simulated in the absence of a SAM ("solution-dense" and "solution-sparse"), the R_{gyr} values were equivalent, consistent with a convergent structural evolution of the two systems (with their distinctly different initial coordinates for the waters). On the other hand, the RMSDX values for these two systems differed by a large margin (25%), which indicates that the two systems certainly did not share an equivalent structural evolution. This is an excellent example of the importance of the initial conditions for an MD simulation. Moreover, it suggests that for such complex systems, averaging over a number of trajectories from a number of initial configurations might be required to produce the most reliable results, given the necessarily limited duration of the trajectories.

Heme orientation angle

In the third column of Table 3 we report the "heme angle," which characterizes the orientation of the protein molecule upon the SAM surface. (Because the protein is tethered to the SAM by means of a covalent disulfide bond to its unique surface cysteine residue, we expect that the orientation of the protein with respect to the SAM should be well defined or "vectorial." This "vectorial orientation" is preserved even allowing for azimuthal averaging about the normal to the monolayer plane, which could be either static or dynamic within the ensemble of cytochrome *c* molecules covalently tethered to the SAM surface, as described in detail in Edwards et al., 2000). This quantity is defined as the angle between the normal vector to the plane of the protein's heme group and the normal vector to the plane of the SAM (i.e., the *x-y* plane of the simulation coordinate frame). At each instant of time during an MD trajectory, the heme plane is defined in terms of the 20 carbon atoms of the porphyrin ring, as follows: the normal vector to this plane is taken to be the average of five normal vectors, each obtained using the coordinates of a set of four carbon atoms spaced evenly (every 90°) around the ring, via the cross-product of the two diagonal in-plane interatomic vectors. Of course, for the two simulated systems without a SAM, the heme angle has no meaning, and no value is given in the table. For the other systems, in each case, the initial configuration (after energy minimization) placed the protein such that the heme angle was ~65°.

The results in Table 3 seem to indicate that the heme angle is relatively insensitive to the polarity of the underlying SAM, as long as the protein is fully hydrated and the heme iron atom is six-coordinate ("nonpolar-wet" and "polar-wet"). On the other hand, for these same systems with low hydration ("nonpolar-damp" and "polar-damp"), the heme angle for the protein on the uncharged-polar SAM is ~4° greater than for the protein on the nonpolar SAM. Furthermore, the "polar-crystal" system does demonstrate a heme angle that is actually ~8° greater than that of the "nonpolar-wet" system, again indicative of the importance of the choice of the initial conditions for the simulation. Meanwhile, for the "nosulfur" systems, the heme angle for the protein on the polar SAM is ~12° greater than for the protein on the nonpolar SAM. The earlier work of Tobias et al. (1996) demonstrated an apparent combination of these effects to an even larger degree: the heme angle in the "polar-dry" simulation was a full 30° greater than that of the "nonpolar-dry" simulation. Much like the RMSDX analysis, these results appear to indicate the effect of water in screening the protein-SAM interaction. In addition, there is a rather profound effect on the heme angle due to the choice of iron coordination model, as one might expect from such a local influence.

The heme angle is an interesting quantity to calculate because it may be directly compared with experimental measurements. Using the technique of polarized optical absorption spectroscopy, Edwards et al. (2000) found a mean heme tilt angle of 59° ± 2° for yeast cytochrome *c* on a nonpolar SAM and 62° ± 3° on an uncharged-polar SAM. Tronin et al. (2002), using a zinc-porphyrin yeast cytochrome *c* and total internal reflection fluorescence spectroscopy, found that the mean tilt angle was 5° to 8° greater for the uncharged-polar SAM than for the nonpolar SAM; both

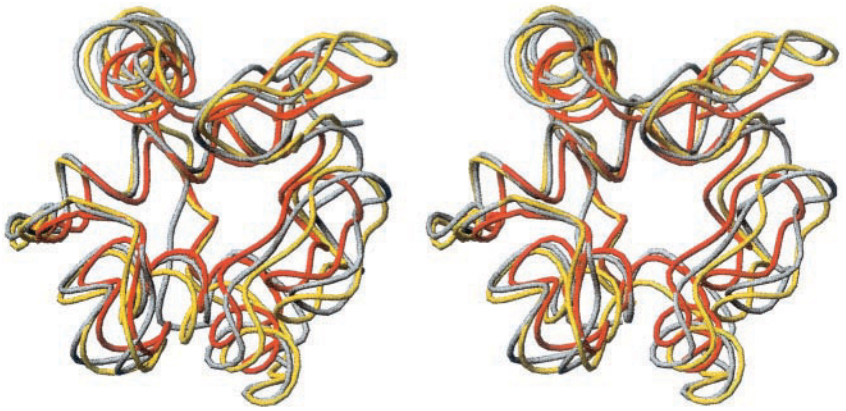

FIGURE 4 Stereographic view of three protein backbone structures: the x-ray crystal structure (1YCC) used as the initial structure for the simulations is shown in gray, an average structure over 100 ps of the "nonpolar-wet" simulation is shown in yellow, and an average structure over 100 ps of the "polar-wet" simulation is shown in red. The two MD structures have each been superimposed upon the crystal structure by a least-squares fitting of the C_α coordinates.

systems exhibited rather narrow orientational distributions but with mean tilt-angle values significantly smaller than for the iron-porphyrin yeast cytochrome *c* noted above. The results of the simulations reported here are in reasonably good agreement with these experimental measures.

Protein secondary structure

It is interesting to investigate the structure of the protein backbone in greater detail. Fig. 4 shows a superposition of three structures in a stereographic ribbon representation: the cytochrome *c* crystal structure (1YCC), a time-averaged structure from the "nonpolar-wet" system, and a time-averaged structure from the "polar-wet" system. One can see that overall, the secondary structure is essentially preserved—certainly no major conformational changes are taking place. As might be expected, the α-helical regions are most similar among the structures, whereas the loop regions show the greatest differences. Fig. 5 shows another superposition of three structures in a stereographic ribbon representation: the cytochrome *c* crystal structure (1YCC), an average of solution NMR structures (1YFC) (Baistrocchi et al., 1996), and a time-averaged structure from the "solution-dense" system. Here we see again that relative to its starting coordinates, the solution simulation does not produce major conformational changes—the α helices are barely altered, and the loop regions show moderate differences. We thought that perhaps the solution simulation would evolve from the crystal structure to something more similar to the solution NMR structure; however, this was not observed. In fact, the differences between the two experimental structures are significantly smaller than the differences between either of those structures and the "solution-dense" simulation structure.

In Fig. 6, we see the situation revealed more quantitatively. The three simulation structures considered here do differ from the crystal structure throughout the primary sequence, but the differences are most pronounced near each end and in the loop region of residues 23 through 31. (Note that our numbering scheme labels the first residue of yeast cytochrome *c* as 1 and the last as 108.) Furthermore, it should be noted that because the largest differences occur in the same parts of the sequence for all three of these simulated systems (i.e., with a nonpolar SAM, a polar SAM, and without a SAM), it appears that the presence of hydration water in the system has a more profound role in modifying the secondary structure than does the presence (or absence) of a soft surface. However, over a large majority of the sequence, the largest differences are observed for the uncharged-polar SAM and the smallest differences

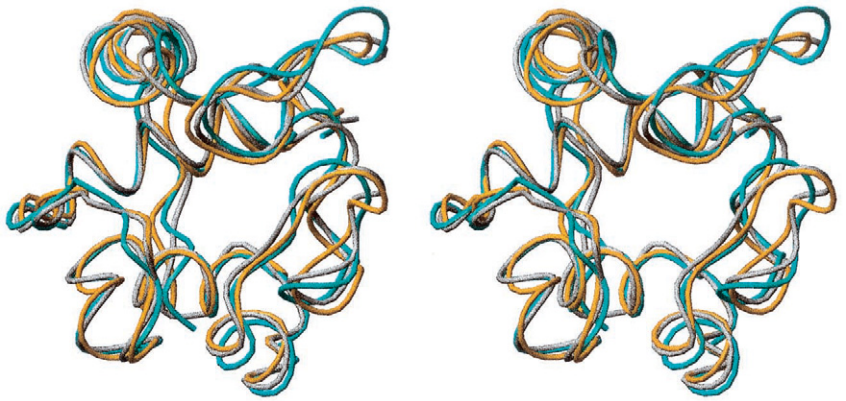

FIGURE 5 Stereographic view of three protein backbone structures: the x-ray crystal structure (1YCC) used as the initial structure for the simulations is shown in gray, the average of a family of 20 solution NMR structures (1YFC) is shown in yellow, and an average structure over 100 ps of the "solution-dense" simulation is shown in cyan. The NMR and MD structures have each been superimposed upon the crystal structure by a least-squares fitting of the C_α coordinates.

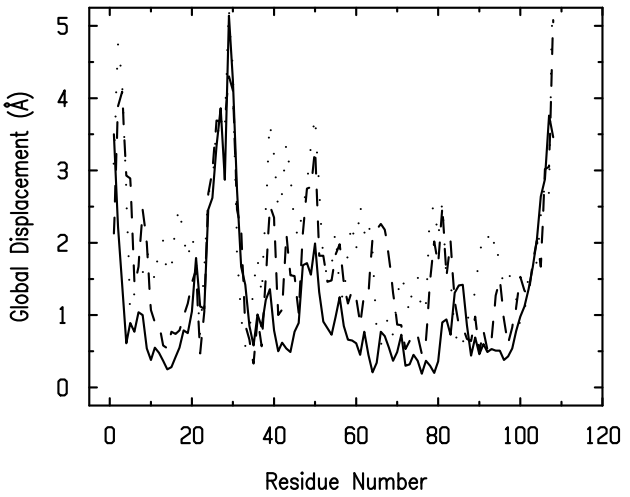

FIGURE 6 Global displacement with respect to the 1YCC crystal structure for 100-ps average structures from three simulated systems: "nonpolar-wet" (*dashed*), "polar-wet" (*dotted*), and "solution-dense" (*solid*) as a function of residue number along the peptide chain. Global displacement for a given residue is defined as the distance between the residue's corresponding C_α coordinates from two structures after minimizing the overall deviation between the structures by a least-squares fitting of all the C_α coordinates.

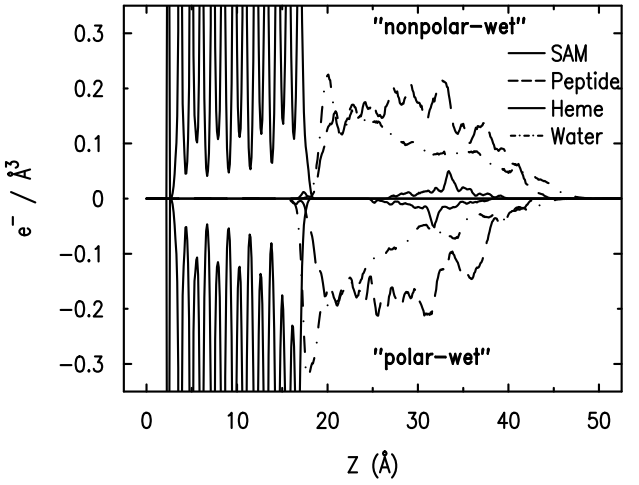

FIGURE 7 Electron density profiles for components of two simulation systems. The upper one-half of the figure shows the electron densities of the SAM (*solid*), the peptide portion of the protein (*dashed*), the heme group portion of the protein (*solid*), and the water (*dot-dashed*) for the "nonpolar-wet" system, averaged over the final 200 ps of the MD trajectory. The lower one-half of the figure shows the same information, vertically inverted for clarity of juxtaposition, for the "polar-wet" system, also averaged over the final 200 ps of the trajectory.

for the solution, with the nonpolar SAM intermediate between these two cases.

System profile structures

Another interesting line of investigation is to look at the profile structures of various systems. (The profile structure is the projection of the three-dimensional structure of the system parallel to the monolayer plane onto an axis normal to the monolayer plane averaged over time.) This analysis becomes particularly important when trying to make a connection between simulation and experimental work using x-ray or neutron interferometry. In Fig. 7, we show the electron density for various component parts of the two canonical simulation systems. Several observations are immediately apparent. First, it is clear that both SAMs are highly ordered. Second, one can see that on the nonpolar SAM, the protein and the water are essentially excluded from the region of space occupied by the SAM; conversely, on the polar SAM, both the protein and the water do appear to penetrate into the region of the SAM endgroups. Further, it is clear that the entire protein structure sits $\sim$2 Å "lower" (closer to the SAM) on the polar SAM than on the nonpolar SAM; this appears completely consistent with (and explainable by) the interpenetration of the protein into the SAM as opposed to any profound "flattening" of the protein. Finally, it is clear that the water in the "polar-wet" system largely shifts toward the SAM surface; this effect is present, but to a much lesser degree, in the "nonpolar-wet" system.

These results from the simulations, regarding the time-averaged position of the cytochrome *c* molecule relative to the SAM surface, are fully consistent with the experimental results from x-ray and neutron interferometry on these nonpolar and uncharged-polar SAM systems as described in Kneller et al. (2001).

To get a feeling for the effect of the protein upon the SAM structure, we show (in Fig. 8) an edge-on snapshot of the two canonical systems, along with profile distributions for the SAM endgroups. From the snapshots, it is apparent that the topmost (endgroup) layer of the SAM is much more vertically disordered in the "polar-wet" system. In the profile plots, we have divided the SAM endgroups into two equal populations: those endgroups that are "under" the SAM and those that are not. It is clear that the disorder in the profile of the SAM endgroups is (in both cases, but particularly so for the polar SAM) due to the interaction with the protein.

To further investigate the specific nature of the interaction between the surfaces of the SAM and the protein, we did a statistical analysis of the two canonical systems to determine which atoms within the protein were closest to the SAM. This was measured as an average over the final 400 ps of each trajectory. It turns out that there was indeed a distinct difference between the interactions with the uncharged-polar surface and the nonpolar surface. For the "polar-wet" system, we found that the five atoms that were closest to the protein were the CYS-107 sulfur (which, as noted above, was covalently bonded to the SAM) and four oxygen atoms (from Phe-41, Gly-42, Lys-104, and Lys-

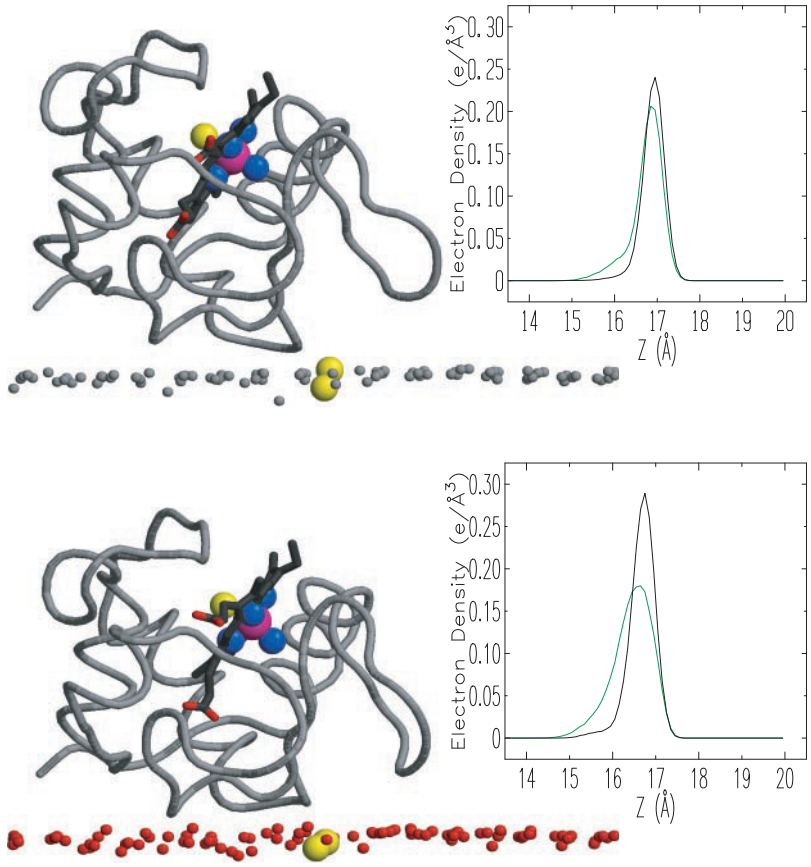

FIGURE 8 (*Left side*) Snapshots of the "nonpolar-wet" (*upper*) and "polar-wet" (*lower*) systems, showing the SAM endgroups, the protein backbone, the heme group, and the disulfide tether between the protein and SAM. (The waters, which bathe the protein and the SAM surface, have here been omitted for clarity.) The color scheme is carbon in gray, nitrogen in blue, oxygen in red, sulfur in yellow, and iron in magenta. (*Right side*) Electron density profiles of the SAM endgroups for the "nonpolar-wet" (*upper*) and "polar-wet" (*lower*) systems. For each system, the endgroups are divided into two equal populations—those that are beneath the protein (*green curves*) and those that are not (*black curves*).

105). These four oxygens each had a partial charge of −0.55, and each was observed to remain closely associated with a specific hydroxyl endgroup hydrogen atom over a timescale of 400 ps. Thus, it is clear that a number of protein residues are tightly bound to specific chains in the polar SAM via hydrogen bonding. Conversely, for the "nonpolar-wet" system, in the absence of any partial charges on the methyl endgroups, no hydrogen bonding occurs between the protein and the SAM. Analyzing the specific interatomic interactions for the same four oxygen atoms of the protein, we found that they did not have any particular associations; there was some evidence of hydrogen bonding with water molecules, but the protein-SAM interactions were nonspecific.

Water profiles

Another interesting property of these simulations is the profile structure of the water molecules. Fig. 9 shows the water profiles for the "nonpolar-wet" and "nonpolar-damp" systems, whereas Fig. 10 shows the water profiles for the "polar-wet" and "polar-damp" systems. In each case, an additional trace is drawn (in red), to represent the profile of the "damp" system (with only 100 waters) scaled up to the same amplitude as the "wet" system (with 500 waters). The water profiles shown are averages over the final 200 ps of each trajectory. (As mentioned above, most of the simulated systems required from 600 to 800 ps for the water profiles to equilibrate.) For the two systems on the nonpolar SAM, the simulated water profiles have a relatively similar shape—the "nonpolar-wet" profile is rather flat, except for a peak near the SAM surface and a slight deficit of water on the far (top) side of the protein; the "nonpolar-damp" profile is also relatively flat with one significant valley of dryness and no obvious edge effects. This seems to indicate that the water associates more strongly with the protein than with the nonpolar SAM. For the two systems on the polar SAM, the simulated water profiles have distinctly different shapes—the "polar-wet" profile shows a very large excess of water near the SAM and a definite decrease in the hydration of the upper parts of the protein; the "polar-damp" system also shows an excess of water near the SAM, but the effect of the SAM on the water profile is much shorter ranged. This seems to indicate that the water associates more strongly with the polar SAM than with the protein. It appears that there is a tendency for a certain minimal amount of water to remain associated with the protein, even in the presence of a polar SAM. This amount is actually less than that required to form a monolayer of water covering the exposed part of the protein, indicating that perhaps only the protein's exposed polar sidechains (and not the nonpolar ones) are able to compete for water with the polar SAM. In

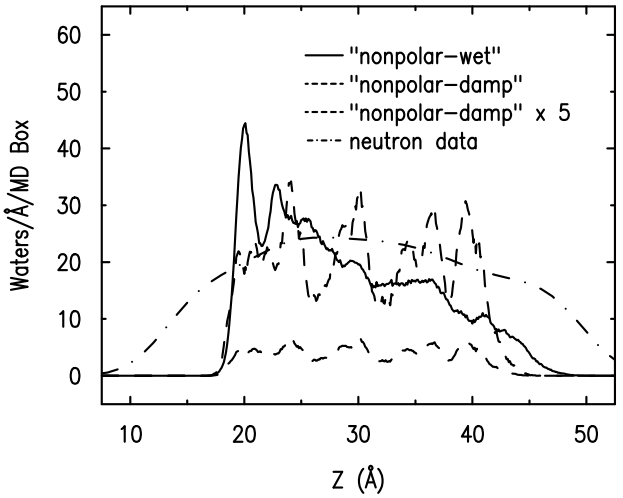

FIGURE 9 Water profile densities, from simulation and experiment, for systems with a protein film deposited upon a nonpolar SAM. We show the profiles for the "nonpolar-wet" (*solid*) and "nonpolar-damp" (*dashed*) simulations; also shown (*dashed*) is the "nonpolar-damp" curve scaled up by a factor of five; also shown (*dot-dashed*), for qualitative comparison, is the result from a neutron reflectivity experiment (Kneller et al., 2001) with the amplitude of the curve scaled arbitrarily.

addition, the water profiles at the 2 mole ratios studied in the case of the uncharged-polar SAM show substantially more pronounced (larger amplitude) features across the protein profile than do those in the case of the corresponding nonpolar SAM.

These results for the water distribution profiles from the simulations are only roughly consistent with the experimental results from neutron interferometry on these nonpolar and uncharged-polar SAM systems as described in Kneller et al. (2001). In that work, the amount of hydrating water was intermediate between the two cases investigated in our simulations. The experimental water profile for the uncharged-polar SAM case showed three pronounced features (as limited by the spatial resolution), whereas (at similar resolution) the experimental profile for the nonpolar SAM case was relatively uniform (as also shown here in Figs. 9 and 10). At this stage of our work, both with these simulations and neutron interferometry studies of various hydration states for the monolayer systems, it appears most likely that the models for the SAMs may be the origin of the discrepancies, because the simulated SAMs are significantly more ordered than their experimental counterparts.

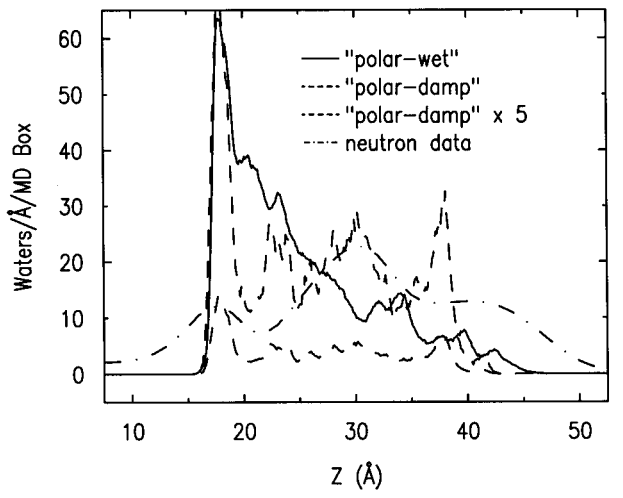

FIGURE 10 Water profile densities from simulation and experiment for systems with a protein film deposited upon a polar SAM. We show the profiles for the "polar-wet" (*solid*) and "polar-damp" (*dashed*) simulations; also shown (*dashed*) is the "polar-damp" curve scaled up by a factor of five; also shown (*dot-dashed*), for qualitative comparison, is the result from a neutron reflectivity experiment (Kneller et al., 2001) with the amplitude of the curve scaled arbitrarily.

CONCLUSIONS

To better understand the nature of protein-membrane interactions, we have performed MD computer simulations on a model system based on the interaction of cytochrome *c* with a soft organic surface, either nonpolar or uncharged-polar in polarity, including a number of variations. We have analyzed the resulting structures and compared the results among one another and with respect to relevant experimental measurements. Our findings are summarized below.

The protein's overall size, manifest via its radius of gyration (R_{gyr}), is influenced by several factors. The R_{gyr} tends to be slightly larger upon interaction with an uncharged-polar SAM surface than with a nonpolar SAM surface and also tends to be larger in the presence of more water; these observations may be explained by favorable interactions of the protein's polar residues with external polar groups presented by a SAM's endgroups and/or solvating water. We also see an increase in the R_{gyr} upon breaking the bond between the heme iron atom and the Met-85 sulfur atom, which is presumably due to the resulting slight relaxation of the protein backbone upon removal of a bonding constraint. We also observe an increase in the R_{gyr} at lower temperature, which we interpret as an effect of the anisotropy of the system. The protein's overall shape, manifest via its eccentricity, is also influenced by these environmental factors. Its eccentricity is greater on the uncharged-polar SAM surface than on the nonpolar SAM surface, whereas its eccentricity in both cases is larger than for the protein in single crystals. Similarly, the difference in the protein's eccentricity on the two different SAM surfaces is twice as large in the absence of hydrating water.

The "RMSDX" is a quantity that measures the deviation of the protein backbone from the x-ray crystal structure. We find that this deviation is greater on average over the protein's sequence for the uncharged-polar SAM than for the nonpolar SAM. It also increases significantly upon breaking the iron-sulfur bond and increases as well in the absence of water. It is apparent that the presence of water serves as a

"screen" that reduces the interaction between the protein and the SAM. Numerical analysis of this quantity also shows that in the absence of a SAM, different equilibrium protein structures may arise simply due to differences in the initial coordinates used for the waters.

We characterize the orientation of the protein upon the SAM by the angle between the plane of the heme group and the plane of the SAM. This "heme angle" is strongly influenced by the choice of model for the heme iron atom coordination; it is also affected, to a lesser degree, by the amount of water present. The results found here do compare favorably with optical linear dichroism measurements of similar systems.

Casual inspection as well as detailed numerical analysis reveals that the overall secondary structure of the protein, and in particular the α-helical regions, are well preserved across all the system variations investigated. The structural variations between systems are concentrated at the ends of the primary sequence and in one of the loop regions. We further deduce that the presence of water is more important to the secondary structure than the polarity of the SAM surface with which it interacts.

Analysis of the systems' so-called profile structures provides a good deal of information. First, we see that the protein and water remain excluded from the nonpolar SAM, whereas the polar SAM demonstrates significant interpenetration of the protein and water. Second, we observe that the disorder present in the profile structure of the SAM endgroups is clearly due to the direct interaction of the SAM with the protein. Looking specifically at the water distribution, we see that the polar SAM competes with the protein for water association, i.e., with a limited amount of water, some but not all of the protein's surface residues remain hydrated. Finally, we find that the different time-averaged positions of the cytochrome *c* protein relative to the SAM surface in these profile structures are in good agreement with the experimental profiles derived from both x-ray and neutron interferometry, and our water profiles are in rough agreement with those derived from neutron interferometry.

In summary, given the reasonable degree of agreement between the simulations and the relevant experimental results, the larger perturbation of the cytochrome *c* structure induced by its interaction with the uncharged-polar SAM surface, as compared with its interaction with the nonpolar SAM surface and in isotropic aqueous solution, appears to arise from the hydrogen bonding of several of its surface residues with the SAM's hydroxyl endgroups. This perturbation occurs presumably because these solvating hydroxyl endgroups are confined to lie within a thin slab on the planar surface of the SAM, unlike those of water solvating the cytochrome *c* surface in the nonpolar SAM and isotropic aqueous solution cases.

This work was supported by the National Institutes of Health grant GM33525 and the NSF/MRSEC grant DMR 00–79909.

REFERENCES

Aleby, S., and E. von Sydow. 1960. The crystal structure of methyl stearate. *Acta Crystallogr.* 13:487–492.

Allen, M. P., and D. J. Tildesly. 1989. Computer Simulation of Liquids. Oxford University Press, New York.

Amador, S. M., J. M. Pachence, R. Fischetti, J. P. McCauley, Jr., A. B. Smith, I. I. I., and J. K. Blasie. 1993. Use of self-assembled monolayers to covalently tether protein monolayers to the surface of solid substrates. *Langmuir.* 9:812–817.

Baistrocchi, P., L. Banci, I. Bertini, P. Turano, K. L. Bren, and H. B. Gray. 1996. Three-dimensional solution structure of saccharomyces cerevisiae reduced iso-1-cytochrome *c*. *Biochemistry.* 35:13788–13796.

Brooks, B. R., R. E. Bruccoleri, B. D. Olafson, D. J. States, S. Swaminathan, and M. Karplus. 1983. CHARMM: a program for macromolecular energy, minimization, and dynamics calculations. *J. Comp. Chem.* 4:187–217.

Buckner, J. K., and W. L. Jorgensen. 1989. Energetics and hydration of the constituent ion pairs of tetramethylammonium chloride. *J. Phys. Chem.* 111:2507–2516.

Chupa, J. A., J. P. McCauley, Jr., R. M. Strongin, A. B. Smith, I. I. I., J. K. Blasie, L. J. Petticolas, and J. C. Bean. 1994. Vectorially-oriented membrane protein monolayers: profile structures via x-ray interferometry/holography. *Biophys. J.* 67:336–348.

Delamarche, E., H. Biebuyck, B. Michael, G. Sundarababu, H. Sigrist, H. Wolf, and H. Ringsdorf. 1995. STM analysis of cytochrome *c* immobilized on self-assembled monolayers on gold. *In* Procedures in Scanning Probe Microscopies. R. J. Colton, A. Engel, J. E. Frommer, H. E. Gaub, A. A. Gewirth, R. Guckenberger, J. Rabe, W. M. Heckl, B. Parkinson, editors. John Wiley and Son, Chichester, UK.

Edmiston, P. L., J. E. Lee, S. S. Cheng, and S. S. Saavedra. 1997. Molecular orientation distributions in protein films: I. Cytochrome *c* adsorbed to substrates of variable surface chemistry. *J. Am. Chem. Soc.* 119:560–570.

Edwards, A. M., K. Zhang, C. E. Nordgren, and J. K. Blasie. 2000. Heme structure and orientation in single monolayers of cytochrome *c* on polar and nonpolar soft surfaces. *Biophys. J.* 79:3105–3117.

Frauenfelder, H., H. Hartmann, M. Karplus, I. D. Kuntz, Jr., J. Kuriyan, F. Parak, G. A. Petsko, D. Ringe, R. F. Tilton, Jr., M. L. Connolly, and N. Max. 1987. Thermal expansion of a protein. *Biochemistry.* 26:254–261.

Hautman, J., and M. L. Klein. 1992. An Ewald summation method for planar surfaces and interfaces. *Mol. Phys.* 75:379–395.

Jorgensen, W. L. 1986. Intermolecular potential functions and Monte Carlo simulations for liquid sulfur compounds. *J. Phys. Chem.* 90:6379–6388.

Jorgensen, W. L., J. Chandrasekhar, J. D. Madura, R. W. Impey, and M. L. Klein. 1983. Comparison of simple potential functions for simulating liquid water. *J. Chem. Phys.* 79:926–935.

Kneller, L. R., A. M. Edwards, C. F. Majkrzak, N. F. Berk, S. Krueger, and J. K. Blasie. 2001. Hydration state of a single cytochrome *c* monolayer vectorially-oriented at a soft interface investigated via neutron interferometry. *Biophys. J.* 80:2248–2261.

Louie, G. V., and G. D. Brayer. 1990. High-resolution refinement of yeast iso-1-cytochrome *c* and comparison with other eukaryotic cytochromes *c*. *J. Mol. Biol.* 214:527–555.

Martyna, G. J., M. L. Klein, and M. Tuckerman. 1992. Nosé-Hoover chains: the canonical ensemble via continuous dynamics. *J. Chem. Phys.* 97:2635–2643.

Pachence, J. M., S. Amador, G. Maniara, J. Vanderkooi, P. L. Dutton, and J. K. Blasie. 1990. Orientation and lateral mobility of cytochrome *c* on the surface of ultrathin lipid multilayer films. *Biophys. J.* 58:379–389.

Pachence, J. M., and J. K. Blasie. 1987. The location of cytochrome *c* on the surface of ultrathin lipid multilayer films using x-ray diffraction. *Biophys. J.* 52:735–747.

Pachence, J. M., and J. K. Blasie. 1991. Structural investigation of the covalent and electrostatic binding of yeast cytochrome *c* to the surface of various ultrathin lipid multilayers using x-ray diffraction. *Biophys. J.* 59:894–900.

Pachence, J. M., R. F. Fischetti, and J. K. Blasie. 1989. Location of the heme-Fe atoms within the profile structure of a monolayer of cytochrome *c* bound to the surface of an ultrathin lipid multilayer film. *Biophys. J.* 56:327–337.

Reiher, W. E. 1985. Theoretical studies of hydrogen bonding. Ph.D. dissertation. Harvard University, Cambridge, MA.

Ryckaert, J.-P., G. Ciccotti, and H. J. C. Berendsen. 1977. Numerical integration of the Cartesian equations of motion of a system with constraints: molecular dynamics of *n*-alkanes. *J. Comp. Phys.* 23:327–341.

Tobias, D. J., W. Mar, J. K. Blasie, and M. L. Klein. 1996. Molecular dynamics simulations of a protein on hydrophobic and hydrophilic surfaces. *Biophys. J.* 71:2933–2941.

Tobias, D. J., K. Tu, and M. L. Klein. 1997. Assessment of all-atom potentials for modeling membranes: molecular dynamics simulations of solid and liquid alkanes and crystals of phospholipid fragments. *J. Chem. Phys.* 94:1482–1502.

Tronin, A., A. M. Edwards, J. Vanderkooi, and J. K. Blasie. 2002. Orientational distributions for cytochrome *c* on polar and nonpolar soft surfaces by polarized total internal reflection fluorescence. *Biophys. J.* 82:996–1003.

Wang, J., C. J. A. Wallace, I. Clark-Lewis, and M. Caffrey. 1994. Structure characterization of membrane bound and surface adsorbed protein. *J. Mol. Biol.* 237:1–4.

Wood, L. L., S. S. Cheng, P. L. Edmiston, and S. S. Saavedra. 1997. Molecular orientation distributions in protein films: II. Site-directed immobilization of yeast cytochrome *c* on thiol-capped self-assembled monolayers. *J. Am. Chem. Soc.* 119:571–576.